

Minimal conceptual models for tropical cyclone intensification

Michael T. Montgomery^{a1} and Roger K. Smith^b

^a Department of Meteorology, Naval Postgraduate School, Monterey, California, USA

^b Meteorological Institute, Ludwig-Maximilians University, Munich, Germany

Abstract: We examine a hierarchy of minimal conceptual models for tropical cyclone intensification. These models are framed mostly in terms of axisymmetric balance dynamics. In the first set of models, the heating rate is prescribed in such a way to mimic a deep overturning circulation with convergence in the lower troposphere and divergence in the upper troposphere, characteristic of a region of deep moist convection. In the second set, the heating rate is related explicitly to the latent heat release of ascending air parcels. The release of latent heat markedly reduces the local static stability of ascending air, raising two possibilities in the balance framework. The first possibility is that the effective static stability and the related discriminant in the Eliassen equation for the overturning circulation in saturated air, although small, remains positive so the Eliassen equation is globally elliptic. The second possibility, the more likely one during vortex intensification, is that the effective static stability in saturated air is negative and the Eliassen equation becomes locally hyperbolic. These models help to understand the differences between the early Ooyama models of 1968 and 1969, the Emanuel 1989 model, and the later Emanuel models of 1995, 1997 and 2012. They provide insight also into the popular explanation of the WISHE feedback mechanism for tropical cyclone intensification. Some implications for recent work are discussed.

KEY WORDS Tropical cyclone intensification; conventional spin-up mechanism; minimal models, nonlinear boundary layer spin-up mechanism, WISHE feedback mechanism

Date: June 25, 2022; Revised ; Accepted

1 Introduction

Tropical cyclones are fascinating large-scale, organized, convective vortices. Unfortunately, these vortices can inflict serious damage and injury to populated coastal communities. The threat of a rapidly intensifying cyclone near coastal communities and marine assets obviously drives practical interest in these storms. Whereas marked progress has been made over the past few decades in the improvement of tropical cyclone tracks, accurate prediction of cyclone intensification remains a considerable challenge (Rogers et al. 2006 and sequel¹).

The main reason for the disparity of progress on these two facets of the cyclone prediction problem is that cyclone tracks depend principally on the large-scale flow in which the vortex is embedded. Improvements in track forecast have resulted from the improved representation of the large-scale environmental flow around the vortex by global forecast models. In contrast, the intensification of a tropical cyclone appears to depend on processes of wide-ranging spatial and temporal scales spanning the large-scale environment, vigorous cumulonimbus updrafts, small-scale turbulence, coalescence of water droplets into rain, evaporation of water from falling rain drops and from

breaking waves under high speed conditions at the sea surface, etc.

Although high spatial resolution (down to order 100 m horizontal grid spacing) and machine learning seem to be the emphasis for obtaining current scientific support to pursue research on tropical cyclone intensification, it is difficult to imagine real progress being made without a commensurate quantum leap in theoretical understanding accompanied by the development of a robust conceptual model that is capable of incorporating the wide-ranging scales thought to be important for improving intensity forecasts.

Since the early 1990's, the WISHE feedback mechanism has been the widely accepted theory to explain tropical cyclone intensification (e.g., Zhang and Emanuel 2016). As an example, Ruppert et al. (2020) begin their study by pointing out that:

“A long history of research indicates that TCs intensify through the WISHE feedback ..., whereby the rate of evaporation increases with surface wind speed.”

However, nowhere in Ruppert et al. is the WISHE feedback process clearly articulated. Rather, WISHE appears to be largely associated with the formula for the evaporation of moisture at the air-sea interface, which is proportional to the near-surface wind speed. Similar ambiguities arise in studies of convective self-aggregation (e.g. Muller and Roms 2018, p2), where the WISHE *mechanism* appears

¹Correspondence to: Prof. Michael T. Montgomery, Dept. of Meteorology, Naval Postgraduate School, Monterey, California, 93943, USA. E-mail: mtmontgo@nps.edu

¹<https://www.nhc.noaa.gov/verification/verify5.shtml>

to be associated with surface flux feedbacks that “connect enhanced surface winds to enhanced surface fluxes.”

In their elegant review of large-scale circulations in convective atmospheres, Emanuel *et al.* (1994) state that:

“Tropical cyclones are quasi-balanced, warm-core systems. They are premier examples of systems arising from WISHE.”

They articulate vortex amplification by first noting that:

“for amplification to occur, the troposphere must become nearly saturated on the mesoscale in the core. When this happens, the vertical entropy distribution no longer has a prominent minimum and there is no low entropy air for downdraughts to import to the subcloud layer. The effective stratification approaches zero in this case, and Ekman pumping becomes inefficient in cooling the core. ... Now the enhanced surface fluxes associated with strong surface winds near the core can actually increase the subcloud-layer entropy and thus the core temperature. The WISHE process results now in a positive feedback to the warm-core cyclone, and the system amplifies.”

This amplification argument is based on thermodynamics and energetics wherein the increase in core temperature, in conjunction with the positive diabatic heating rate, is regarded as the source for available potential energy, which then generates an increase in kinetic energy of the vortex. The energetics here are presumably global energy quantities spatially integrated over the entire vortex. If this were not the case and these energy quantities were intended to represent local properties, then energy transport terms would need to be included to give a complete and consistent account of the system energetics (Anthes 1974; Smith *et al.* 2018b). Much less is known about the specifics of these transport terms during vortex spin up. Thus, the implied association of an increase in global kinetic energy with an increase of the maximum tangential wind, V_{max} , is an *ad hoc* assumption that will not apply in general. We would argue that a consistent and defensible dynamical explanation for the *amplification of V_{max}* is required.

An explanation of the spin up of V_{max} using the WISHE feedback viewpoint is underpinned only by rather complex models formulated in potential radius coordinates (Emanuel 1995, 1997, 2003), with the simplified model presented in the latter two papers based on some dubious assumptions (Montgomery and Smith 2014). In particular, spin up in the model depends crucially on the radial gradient of an *ad hoc* parameter, β , which is introduced to mimic the deleterious effects of convective downdraughts into the boundary layer yet is not derivable from the governing equations. The parameter β seems to be a legacy from the invocation of convective downdraughts noted in the foregoing Emanuel *et al.* explanation. Recognizing the

ad hoc nature of this formulation, Emanuel (2012) reformulated the model to avoid the introduction of β , but this has not led to a revised theory for the WISHE feedback and the new model has its own issues (Montgomery and Smith 2019; Montgomery *et al.* 2019). An outstanding question remains as to whether a minimal dynamical model exists that can transparently explain the essential physics of the WISHE feedback mechanism?

The WISHE feedback mechanism has become not only the widely accepted theory to explain the intensification of tropical cyclones, it is extensively invoked as the mechanism to explain the intensification process of occasional tropical-cyclone-like low pressure systems over the Mediterranean, so called medicanes (Emanuel 2005; Carrió *et al.* 2017; Miglietta *et al.* 2020; Miglietta and Rotunno 2019). Since, as noted by Montgomery *et al.* (2015), there is confusion in the literature on precisely what constitutes the WISHE mechanism, it is pertinent to examine how the mechanism is currently articulated in the medicane literature.

The recent explanation by Miglietta and Rotunno (2019) that applies to tropical cyclones as well highlights the central issue. On page 559 they say:

“We have established, using a numerical model, that a hurricane-like vortex may grow as a result of a finite amplitude instability in an atmosphere which is neutrally stable to the model’s moist convection. *The mechanism* (our emphasis), which is a form of air-sea interaction instability, operates in such a way that wind-induced latent heat fluxes from the ocean lead to locally enhanced values of θ_e in the boundary layer which, after being redistributed upward along angular momentum surfaces, lead to temperature perturbations aloft. These temperature perturbations enhance the storm’s circulation, which further increases the wind-induced surface fluxes, and so on. The tropical cyclone will continue to intensify so long as boundary-layer processes permit steadily increasing values of θ_e near the core or until the boundary layer there becomes saturated.”

In this explanation, θ_e refers to the reversible equivalent potential temperature. In the remainder of this article, we use θ_e to denote the pseudo-equivalent potential temperature.

The explanation raises important questions. How does a redistribution aloft of locally enhanced values of θ_e in the boundary layer along (absolute) angular momentum surfaces lead to the inward movement of these surfaces above the boundary layer? This inward movement is a necessary requirement for the tangential velocity component to increase (e.g. Smith and Montgomery 2016). And how do the “temperature perturbations enhance the storm’s circulation”? In the Emanuel (1995), Emanuel (1997) and Emanuel (2012) theories, it is assumed that there is no local buoyancy associated with temperature perturbations, i.e.,

the overturning circulation is assumed to be exactly moist neutral (see Section 2.4 for more on this point). As far as we know, none of the papers on medicanes that use the term WISHE (including that of Emanuel 2005) have provided a clear physical articulation of the WISHE feedback mechanism, including the amplification of V_{max} .

Two more recent papers by Zhang and Emanuel (2016) and Emanuel (2019) add further confusion by apparently redefining the ‘‘WISHE feedback process’’ as simply the formula relating the increase of surface enthalpy flux to the surface wind speed and to the degree of thermodynamic disequilibrium near the surface, without explaining how the increased fluxes lead to an increase in surface wind speed as in earlier studies (see e.g. Montgomery and Smith 2014, figure 6 and related discussion). Although section 2 of Zhang and Emanuel (2016) presents an example of a feedback process, it is unclear how this example relates to the purported WISHE intensification process for a tropical cyclone (see Appendix of Kilroy et al. 2022).

Recent work by Zhu et al. (2021) has found that intensification and track forecasts of recent North Atlantic Hurricanes are significantly improved when the Hurricane Analysis and Forecast System (HAFS), used by the National Atmospheric and Oceanographic Administration (NOAA) team, is improved to better estimate the static stability in clouds associated with the intense turbulent mixing in the eyewall and rainband regions. The study specifically found that:

‘‘... sub-grid scale (SGS) turbulent transport above the PBL (Planetary Boundary Layer, our insertion) in the eyewall plays a pivotal role in initiating a positive feedback among the eyewall convection, mean secondary overturning circulation, vortex acceleration via the inward transport of absolute vorticity, surface evaporation, and radial convergence of moisture in the PBL.’’

The finding that an improved SGS scheme above the PBL helps support the vigor of eyewall convection is not implausible and may highlight a useful way forward to being able to better predict rapid intensification events in real-world cases. If this is indeed the case, then it would seem important to understand the underlying reason for the improved predictions. The authors attribute this improved performance (p17) to the ‘‘kicking off’’ of a ‘‘WISHE-like positive feedback mechanism’’ in the updated modeling system. However, it is unclear precisely what the authors mean by the ‘‘WISHE-like positive feedback mechanism’’ and it seems mysterious, at least to us, why the WISHE-like mechanism kicks in only when the representation of the SGS processes influencing the vertical stability in clouds has been updated. We will return to this study later in Section 5.

In summary, based on the above review, a clear articulation of the WISHE feedback mechanism for the amplification of V_{max} in a tropical cyclone is missing. Without

such an articulation, it is unclear to us how other processes, such as cloud infrared radiation, small-scale mixing or turbulence represented in large-eddy-simulations, interact with the alleged intensification mechanism identified with WISHE.

In this short paper we develop a small hierarchy of minimal, axisymmetric, conceptual models to gain a better understanding of the spin up of the system-scale tangential winds in a tropical cyclone. These models establish a useful framework to understand the relationship between a range of previous minimal models including Ooyama’s nonlinear models and the various models of Emanuel. They provide also a framework for articulating the WISHE feedback mechanism.

2 Minimal conceptual models for vortex intensification

The proposed intensification models to be described are based on the classical axisymmetric Eliassen balance vortex formulation (Shapiro and Willoughby 1982, Schubert and Hack 1982, Wirth and Dunkerton 2006, *et. seq.*), which assumes the flow to be in strict gradient wind and hydrostatic balance. Moreover, it is pertinent to note that the minimal models used by Ooyama and those of Emanuel use an axisymmetric balance formulation, at least above the boundary layer. This formulation is arguably the simplest framework to represent the main elements of tropical cyclone intensification, at least in a first approximation of a slowly evolving vortex, even though it is known that the balance evolution framework does not capture the spin up dynamics in the boundary layer for a realistic tropical cyclone (see Section 2.5) and has solvability issues as the vortex intensifies (see Section 4).

2.1 The general prognostic balance model

The equations for a general, axisymmetric, prognostic balance model formulated in cylindrical r - z coordinates are given in Smith et al. (2018a). The prognostic element is the tendency equation for tangential wind component v :

$$\frac{\partial v}{\partial t} = -u \frac{\partial v}{\partial r} - w \frac{\partial v}{\partial z} - \frac{uv}{r} - fu - \dot{V}, \quad (1)$$

where u and w are the radial and vertical velocity components, t is the time, f is the Coriolis parameter (assumed constant), and $-\dot{V}$ is the azimuthal momentum sink associated with the near-surface frictional stress. The balanced density field is obtained from the thermal wind equation, which has the general form:

$$\frac{\partial \log \chi}{\partial r} + \frac{C}{g} \frac{\partial \log \chi}{\partial z} = -\frac{\xi}{g} \frac{\partial v}{\partial z}, \quad (2)$$

where $\chi = 1/\theta$ is the inverse of potential temperature θ , $C = v^2/r + fv$ is the sum of centrifugal and Coriolis forces

per unit mass, $\xi = f + 2v/r$ is twice the local absolute angular velocity and g is the acceleration due to gravity. This is a first order partial differential equation for $\log \chi$, which on an isobaric surface is equal to the logarithm of density ρ plus a constant, with characteristics $z_c(r)$ satisfying the ordinary differential equation $dz_c/dr = C/g$.

At the heart of the formulation is a second-order partial differential equation for the streamfunction of the secondary overturning circulation ψ , the so-called Eliassen equation. This equation determines the overturning circulation required to keep the primary (tangential) circulation in gradient wind balance and hydrostatic balance in the presence of thermal and tangential momentum forcing that would otherwise destroy such balances. The Eliassen equation takes the general form:

$$\frac{\partial}{\partial r} \left[\gamma \left(N^2 \frac{\partial \psi}{\partial r} - B \frac{\partial \psi}{\partial z} \right) \right] + \frac{\partial}{\partial z} \left[\gamma \left(I_g^2 \frac{\partial \psi}{\partial z} - B \frac{\partial \psi}{\partial r} \right) \right] = g \frac{\partial}{\partial r} (\chi^2 \dot{\theta}) + \frac{\partial}{\partial z} (C \chi^2 \dot{\theta}) + \frac{\partial}{\partial z} (\chi \xi \dot{V}), \quad (3)$$

where $\gamma = \chi/(\rho r)$, $N^2 = -(g/\chi)\partial\chi/\partial\chi$, $I_g^2 = \xi\zeta_a + (C/\chi)\partial\chi/\partial r$, $B = (1/\chi)/\partial(\chi C)/\partial z$, $\zeta_a = \zeta + f$ is the absolute vorticity, $\zeta = (1/r)\partial(rv)/\partial r$ is the vertical component of relative vorticity, $\dot{\theta} = d\theta/dt$ is the diabatic heating rate and $-\dot{V}$ is the tangential component of the frictional force per unit mass. The derivation of this equation is sketched in section 2.2 of [Bui et al. \(2009\)](#). The transverse velocity components u and w are given in terms of ψ by:

$$u = -\frac{1}{r\rho} \frac{\partial \psi}{\partial z}, \quad w = \frac{1}{r\rho} \frac{\partial \psi}{\partial r}. \quad (4)$$

The discriminant of the Eliassen equation, Δ , is given by

$$\Delta = 4\gamma^2 (I_g^2 N^2 - B^2), \quad (5)$$

where $\gamma = \chi/(\rho r)$, and the Eliassen equation is elliptic if $\Delta > 0$.

If the heating rate and frictional forcing are given, and provided that the Eliassen equation is everywhere elliptic, the equation system (1)-(4) may be solved in principle as follows:

- Step (1): Starting with an initial condition for $v(r, z, t)$, say $v(r, z, 0)$, calculate the initial balanced thermal field, characterized by $\chi(r, z, 0)$, from Eq. (2) using, for example, the method outlined by [Smith \(2006\)](#);
- Step (2): Solve the Eliassen equation (3) for $\psi(r, z, 0)$, subject to suitable boundary conditions along all boundaries of the flow domain, checking first that the equation is globally elliptic² using Eq. (5);

²If the equation has regions where $\Delta \leq 0$, it may be possible to obtain a “weak” solution by modifying the coefficients of the highest partial derivatives so that Δ becomes small and positive in this region (see e.g., [Smith et al. 2018a](#); [Montgomery and Persing 2020](#); [Wang et al. 2021](#)).

- Step (3): Calculate the velocity components of the overturning circulation $u(r, z, 0)$ and $w(r, z, 0)$ using Eqs. (4).
- Step (4): Predict the tangential velocity $v(r, z, \Delta t)$ using Eq. (1) at some later time Δt , chosen to be suitably small.

These four steps may be repeated to build the solution for a series of times $t = n\Delta t$, where n is a positive integer.

Some examples of such solutions are discussed by [Smith et al. \(2018a\)](#) and [Smith and Wang \(2018\)](#) in which the heating rate and frictional forcing are prescribed spatial functions with the location of the heating distribution being tied, in general, to a moving M -surface, which is prescribed also. While such solutions prove useful for developing basic understanding, a complete theory would require the heating rate to be linked intrinsically to the vortex dynamics and thermodynamics. One simple way to do this is as follows.

If an ascending air parcel becomes saturated, condensation of water vapour occurs at a rate equal to the material rate-of-change of saturation mixing ratio, r_v^* . The rate of latent heat release is given then by the approximate formula

$$\dot{Q} \approx -L_v w \frac{\partial r_v^*}{\partial z}, \quad (6)$$

where L_v is the latent heat of condensation³.

Since $\partial r_v^*/\partial z$ is related to θ_e^* of the ascending air, the prescription of \dot{Q} is essentially equivalent to a prescription of w where the air is ascending in a deep convective cloud. Typically, in such clouds, \dot{Q} increases in the lower troposphere to reach a maximum somewhere in the mid-troposphere and decreases again in the upper troposphere. Thus, the prescription of such a vertical structure for \dot{Q} implies a similar structure of w in the heated region, consistent with the fact that deep convective clouds are accompanied by mean horizontal convergence in the lower troposphere and mean horizontal divergence in the upper troposphere. It is for this reason that the use of a prescribed heating rate with this vertical structure to represent a region of deep convection produces results that have some degree of realism when used in a zero-order minimal model for tropical cyclone intensification.

2.2 Zero-order model

The prognostic models investigated by [Smith et al. \(2018a\)](#) and [Smith and Wang \(2018\)](#) are arguably amongst the simplest for isolating the dynamical aspects of spin up in the foregoing balance framework. In most of these models, the amplitude of the diabatic heating rate is held fixed in time, but the distribution of heating rate is allowed to contract as the vortex contracts. A range of calculations were carried out there for the frictionless case with prescribed heating and for cases with a simple formulation of surface drag,

³The diabatic heating rate, $\dot{\theta}$ and the latent heating rate \dot{Q} are related by the formula $\dot{\theta} = \dot{Q}/(c_p \pi)$, where π is the Exner function.

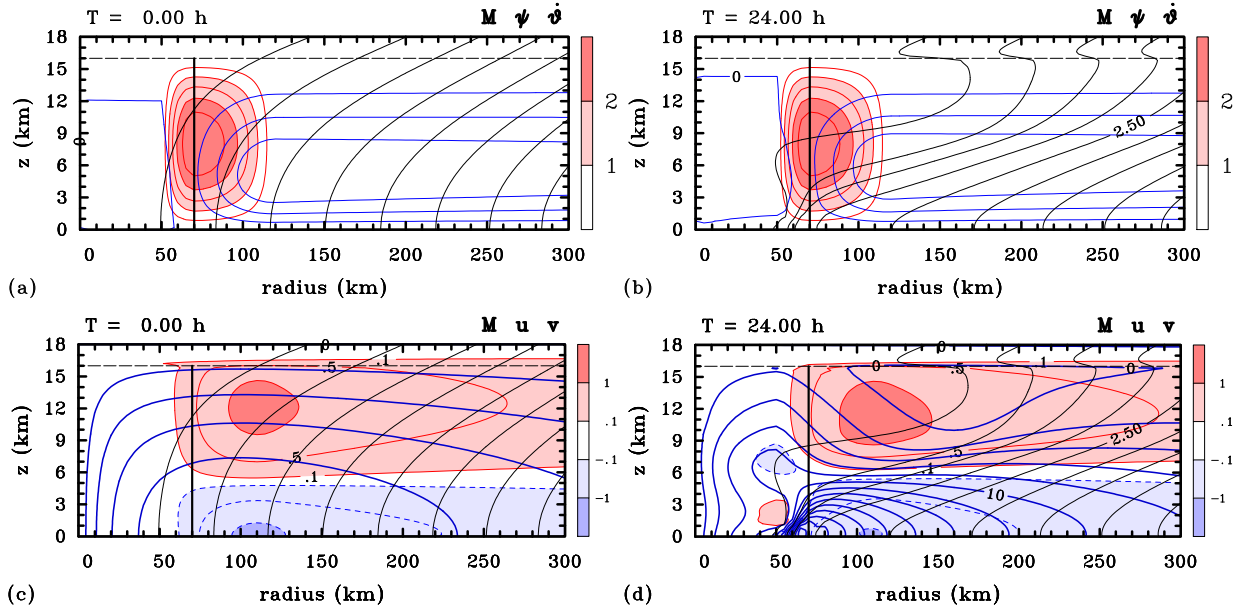


Figure 1. Radial-height cross sections of M -surfaces (thin black curves) superimposed on various quantities for the zero-order model without friction. These quantities include: (a,b) streamlines of the secondary circulation, ψ (blue curves), and diabatic heating rate $\dot{\theta}$ (shaded); (c,d) contours of tangential velocity, v (blue curves), and radial velocity u (shaded). The upper panels are at the initial time and the lower panels are at 24 h. The dashed horizontal line at a height of 16 km indicates the tropopause. The thick vertical line shows the axis of the maximum diabatic heating rate. Contour intervals are: for M , $5 \times 10^5 \text{ m}^2 \text{ s}^{-1}$; for ψ , $1 \times 10^8 \text{ kg s}^{-1}$ for positive values (solid), $5 \times 10^7 \text{ kg s}^{-1}$ for negative values (dashed); for $\dot{\theta}$, 0.5 K h^{-1} ; for u , 0.1 m s^{-1} , 0.5 m s^{-1} and 1 m s^{-1} (negative values dashed); for v , 2 m s^{-1} .

with or without heating. In the zero order model here we will consider first the case without friction in which the heating distribution is held fixed in space (the case designated Ex-US by Smith et al.).

The upper panels of Fig. 1 show radius-height cross sections of the diabatic heating rate and streamfunction of the secondary circulation at the initial time and after 24 hours for this calculation, while the lower panels show the radial and tangential velocity components at these times. In all figures, the M -surfaces⁴ are superimposed. Both times are before the regularization procedure (as discussed by Smith et al. 2018a) is first required at about 30 hours.

As in the Smith et al. calculations, where the heating region moves inwards with a particular M -surface, the flow outside the heating region is quasi-horizontal with inflow in the lower troposphere, below about 5 km, and outflow above this level. The M -surfaces are advected inwards in the lower troposphere, highlighting the classical spin-up mechanism for tropical cyclone intensification, which, in an axisymmetric framework, attributes vortex spin up to the

convectively-induced inward radial advection of absolute angular momentum M at levels where this quantity is materially conserved. Most of the inflow passes through the region of heating and, at low to mid-levels, the flow has a significant component across the M -surfaces in the direction towards decreasing M . In the developing high wind region of the vortex where the inflowing air turns upwards, the vertical advection of M becomes important in spinning up the flow there.

In this solution, both the maximum tangential wind speed, V_{max} , and maximum inflow, U_{min} , occur at, or near, the surface. This is to be expected because V_{max} lies at the surface initially and the convectively-induced inflow remains a maximum close to the surface⁵, within 400 m of the surface at subsequent times. From Eq. (7), the nonzero vertical advection of M just above the surface accounts for the progressive, but small elevation of V_{max} . Thus, the largest inward advection of the M -surfaces occurs just above the surface. The asymmetry in the depths of the inflow and outflow layers is a consequence of mass continuity and the fact that density decreases approximately exponentially with height. The maximum outflow occurs at a height of about 12 km.

If the distribution of diabatic heating rate is allowed

⁴The absolute angular momentum per unit mass $M = rv + fr^2/2$, where r is the radius from a nominal invariant circulation centre, v is the azimuthally-averaged tangential velocity in relation to the centre, and f is the Coriolis parameter, assumed constant, the so-called f -plane approximation. In terms of M , in the case without friction, Eq. (1) may be written in the form

$$\frac{\partial v}{\partial t} = -\frac{u}{r} \frac{\partial M}{\partial r} - \frac{w}{r} \frac{\partial M}{\partial z}. \quad (7)$$

⁵In our prior publication of Smith et al. (2018a), the statement on p3174 (1c) that “ U_{min} occurs at the surface at subsequent times” is not quite accurate. In fact, U_{min} after several hours occurs slightly above the surface and we accordingly retract that statement even though the broad description of the results is still correct.

to move inwards with time, tied to a prescribed M surface, spin up occurs at a slightly increased rate compared with the case when this distribution is held fixed.

2.3 A minimal representation of friction

As explained in section 3.5 of [Smith and Wang \(2018\)](#), the addition of friction in the balance model is somewhat pathological as friction is applied only in the tangential momentum equation. Moreover, while the application of a frictional force in this equation leads to radial inflow, the assumption of gradient wind balance in the friction layer requires frictional effects to be no more than a small perturbation to the balanced flow ([Smith and Montgomery 2008](#)). In contrast, more realistic vortex boundary layers are intrinsically unbalanced (see Section 2.5). With the balance approximation, the inflow is forced by the need to maintain balance in the presence of a frictional force that is trying to destroy balance. This means that the frictionally-driven inflow is present from the initial instant, whereas the boundary layer in the tangential direction is not and requires time to develop. For these reasons, one might describe the representation of friction in a balanced vortex as a *minimal representation of friction*.

2.3.1 Zero-order model with friction only

It is well known that the primary mechanism of spin down of realistic high-Reynolds' number vortices is associated with the outward radial advection of absolute angular momentum above the surface-based friction layer brought about by the secondary overturning circulation induced by friction and not by the direct diffusion of tangential momentum to the lower boundary ([Greenspan and Howard 1963](#)). This mechanism is a feature of the spin down of a balanced vortex in the absence of diabatic heating, solutions for which were shown in section 4a of [Smith et al. \(2018a\)](#). If there were no diabatic heating and if the atmosphere is stably stratified, the frictionally-driven inflow would lead to a shallow layer of outflow just above the boundary layer.

Figure 2a shows the initial tangential and radial wind components with the M -surfaces superimposed, while Fig. 2b shows the same fields after 6 hours. As expected, the overturning circulation is weaker and shallower after 6 hours and the maximum tangential velocity has diminished in strength and has become elevated. The lower panels of Fig. 2 show the corresponding vertical velocity at these two times up to a height of 6 km. Of interest is the fact that in the domain shown, the vertical velocity is everywhere positive at both times, with a broad maximum centred at an altitude of 700 m inside the radius of maximum tangential wind (initially 100 km).

2.3.2 Zero-order model with heating and friction

Figure 3 shows radius-height cross sections of the radial and tangential velocity components at the initial time and

after 12 hours for the calculation with heating and friction. As in the case where the heating distribution moves with a prescribed M -surface (section 4e of [Smith et al. 2018a](#)), the largest inflow in the presence of surface friction occurs within the frictional boundary layer, even in this case where gradient wind balance is assumed to hold approximately in the boundary layer as well.

The motivation for examining the case where the heating distribution is held fixed in space is to pave the way for the first-order model discussed below, in which the heating distribution is determined as part of the solution. However, in the presence of friction, the solution where the heating distribution is held fixed in space breaks down a little after 12 hours. What appears to happen in this case is that the shallow frictionally-induced return flow above the boundary layer inside the heating is accentuated by the outflow there driven by the heating. This shallow outflow leads to a rapid increase in the radial gradient of M near the axis of heating and thereby a large radial gradient of tangential velocity and large vorticity. In turn, these large gradients appear to prevent the successive-over-relaxation method for solving the Eliassen equation from converging.

2.4 First-order model

We consider now the possibility of relating the diabatic heating rate to the thermodynamics of the developing vortex, which would enhance the realism of the zero-order models described above. Attempts to do this in an axisymmetric balance framework go back to [Ooyama \(1969\)](#), [Sundqvist \(1970a,b\)](#) and [Emanuel \(1989\)](#). All of these studies incorporated a parameterization for deep convection. Here we begin by adopting a more direct approach based on the equations detailed in Section 2.1.

2.4.1 Mathematical formulation in cloudy regions

In cloudy regions $r_v = r_v^*(p, \chi)$, the substitution for \dot{Q} using Eq. (6), with Eq. (4) used to relate w to ψ , the Eliassen equation takes the form

$$\begin{aligned} & \frac{\partial}{\partial r} \left[\gamma \left(N^2 + \frac{gL_v}{c_p T} \frac{\partial r_v^*}{\partial z} \right) \frac{\partial \psi}{\partial r} - \gamma B \frac{\partial \psi}{\partial z} \right] + \\ & \frac{\partial}{\partial z} \left[\gamma I_g^2 \frac{\partial \psi}{\partial z} - \gamma \left(B - \frac{CL_v}{c_p T} \frac{\partial r_v^*}{\partial z} \right) \frac{\partial \psi}{\partial r} \right] = \frac{\partial}{\partial z} (\chi \xi \dot{V}), \end{aligned} \quad (8)$$

with the new discriminant

$$\Delta = 4\gamma^2 \left[I_g^2 \left(N^2 + \frac{gL_v}{c_p T} \frac{\partial r_v^*}{\partial z} \right) - \left(B - \frac{CL_v}{2c_p T} \frac{\partial r_v^*}{\partial z} \right)^2 \right]. \quad (9)$$

However, where the air is unsaturated, $r_v < r_v^*(p, \chi)$, the Eliassen equation in the form of Eq. (3) remains appropriate. (Of course, Eq. (8) reduces to Eq. (3) if the terms involving latent heat release, which are proportional to L_v , are set to zero.) Clearly, to determine whether or not the air

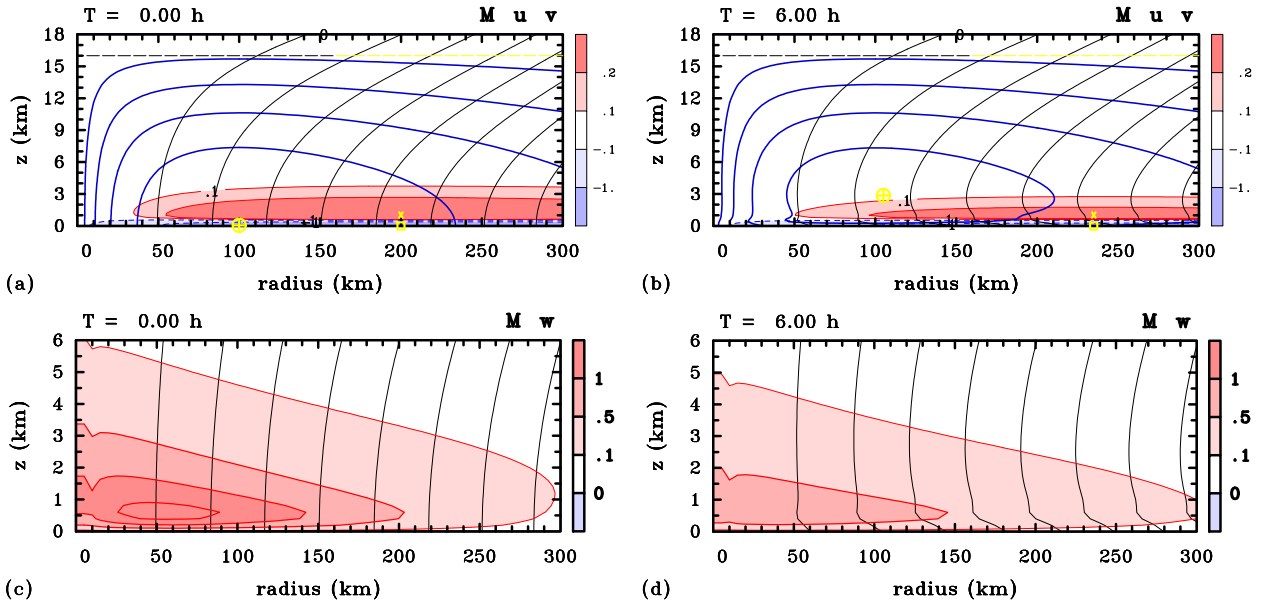


Figure 2. Radial-height cross sections of M -surfaces (thin black curves) superimposed on various quantities for the friction-only simulation. These quantities include: (a,b) contours of tangential velocity, v (blue curves), and radial velocity u (shaded), and (c,d) contours of vertical velocity, w (shaded) up to an altitude of 6 km. The left panels are at the initial time and the right panels are at 6 h. The dashed horizontal line at a height of 16 km indicates the tropopause. Contour intervals are: for M , $5 \times 10^5 \text{ m}^2 \text{ s}^{-1}$; for v , 2 m s^{-1} ; for w , 0.5 cm s^{-1} with the additional contour 0.1 cm s^{-1} shown also. Contours for u are 0.1 m s^{-1} and 0.2 m s^{-1} for positive values, 0.1 and 1 m s^{-1} for negative values. Positive contours are solid, negative contours dashed. The yellow symbols in (a) and (b) indicate the locations of maximum v , (\oplus), maximum u , (\times) and minimum u , (\square)

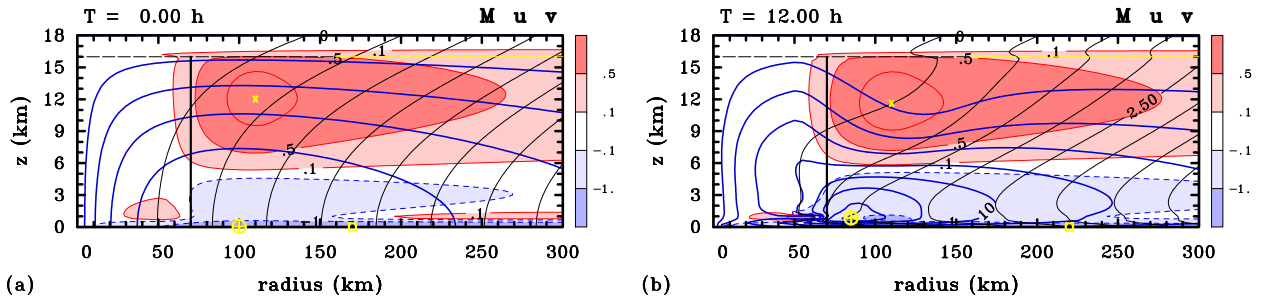


Figure 3. Radial-height cross sections of M -surfaces (thin black curves) superimposed on various quantities for the simulation with heating and friction. These quantities include: contours of tangential velocity, v (blue curves), and radial velocity u (shaded) at (a) the initial time, and (b) 12 hours. The dashed horizontal line at a height of 16 km indicates the tropopause. The thick vertical line shows the location of the maximum diabatic heating rate, which is fixed in time. Contour intervals are: for M , $5 \times 10^5 \text{ m}^2 \text{ s}^{-1}$; for u , 0.5 m s^{-1} , 0.02 m s^{-1} (thin solid contours below 2.5 km height and inside 75 km radius), 1 m s^{-1} for negative values dashed contours; for v , 2 m s^{-1} . The yellow symbols indicate the locations of maximum v , (\oplus), maximum u , (\times) and minimum u , (\square)

is cloudy, we need to introduce a prediction equation for r_v in the first-order model. The influence of surface moisture fluxes would enter through this equation.

Note that, if friction were not included as part of the first-order model (i.e., $\dot{V} = 0$), there would be no forcing terms on the right-hand-side of Eq. (8) and the only solution would appear to be the trivial solution $\psi = 0$. This outcome is supported by physical considerations. Because \dot{Q} is proportional to w , without frictional forcing, a solution starting with no heating initially would not be able to develop heating.

In cloudy regions, where there is pseudo-adiabatic

ascent, $\partial r_v^* / \partial z < 0$, whereupon both terms involving $\partial r_v^* / \partial z$ in Eq. (9) lead to a reduction of Δ . Moreover, in these regions, the coefficient of $\partial^2 \psi / \partial r^2$ in Eq. (8) may be written as

$$g\gamma \left(\frac{1}{\theta} \frac{\partial \theta}{\partial z} + \frac{gL_v}{c_p T} \frac{\partial r_v^*}{\partial z} \right) \approx \frac{\gamma g}{\theta_e^*} \frac{\partial \theta_e^*}{\partial z}, \quad (10)$$

where θ_e^* is the saturation pseudo-equivalent potential temperature. If air parcels were rising without mixing, θ_e^* would be materially conserved and in a steady flow with air parcels rising vertically, $\partial \theta_e^* / \partial z$ would be zero. In this case, the discriminant Δ would be zero or negative. Note that the

quantity $(g/\theta_e^*)/(\partial\theta_e^*/\partial z)$ is the effective static stability in cloudy air.

2.4.2 Qualitative structure of the solutions

In view of the foregoing mathematical results, it is enlightening to examine the qualitative structure of solutions to Eq. (8) in two situations depending on the character of the equation in cloudy air as determined by the sign of Δ .

Case A: Suppose that the effective static stability in saturated air becomes relatively small, but remains sufficient to keep $\Delta > 0$ there, and that $\Delta > 0$ in unsaturated air also. In this case, the Eliassen equation would be globally elliptic and the solutions thereto would be qualitatively similar to those in the case with no heating in the sense that there will be inflow in the layer with friction and outflow above (cf. Section 2.3.1). However, we would expect the reduced static stability in cloudy air to allow for a deeper layer of outflow than in the case with friction only. In support of this conjecture, we show in Fig. 4 a repeat of the calculation with no heating in Section 2.3.1, but with the coefficient of the second-order derivative $\partial^2\psi/\partial r^2$ multiplied by a factor 0.2 at each grid point in a region extending in radius from 20-90 km (centred around the region of maximum ascent in Fig. 2c) and from an altitude of 1 km to 14 km to crudely mimic the effect of reduced static stability on account of presumed latent heat release over the bulk of the troposphere (indicated by a rectangular box in the figure). The upper panels show the same fields as Fig. 2a,b at the initial time and at 6 hours.

As one might have anticipated by invoking the membrane analogy (see e.g., Wang and Smith 2019, section 3), a significant reduction in the coefficient of $\partial^2\psi/\partial r^2$ in the Eliassen equation, i.e., a reduction in the effective static stability, would be expected to lead to a significant increase in the depth to which air would rise as it leaves the boundary layer and therefore a considerable deepening of the layer of outflow above the boundary layer. The calculations shown in Fig. 4 support this supposition: compare for example the upper panels of Fig. 4 with those of Fig. 2. Comparing the lower panels of Fig. 4 with the upper panels shows that the overturning circulation has undergone significant decay in just a 6 hour period.

Case B: In contrast to Case A, suppose the effective static stability becomes negative in cloudy air. In such a region, $\Delta < 0$ and Eq. (8) would be hyperbolic in such regions. In these unstable regions, air parcels would be able to accelerate vertically under their local buoyancy so that the hydrostatic approximation and therefore thermal wind balance would break down. In this most likely scenario, the breakdown of the formulation as a globally elliptic problem is an indication that localized buoyant deep convection is seeking to develop. In particular, the breakdown suggests also that the simple parameterization encapsulated in the formula (6) in conjunction with the hydrostatic

constraint is inadequate to represent such convection. With the hydrostatic approximation, and therefore within the balance framework, air parcels experience no net vertical force to accelerate them vertically and for this reason, the characteristic flow patterns of low-level convergence and upper-level divergence typical of deep convection are unable to develop.

The conclusion from the foregoing analysis is that the simple parameterization given by the formula (6), in conjunction with the imposition of hydrostatic and gradient balance, is unable to facilitate the low-level inflow required to reverse the frictionally-induced outflow in the lower troposphere above the boundary layer, and thereby unable to provide the necessary convergence there for vortex spin up.

2.5 Beyond the minimal representation of friction

Before considering some implications of the foregoing deductions from the first-order model, it is worth remarking on the limitations of the representation of friction in a balance framework (Section 2.3). When a more realistic boundary layer is formulated to include a full radial momentum equation, important nonlinear effects materialize in the ensuing dynamics of vortex spin up. In particular, one finds that the maximum storm-relative tangential wind in the azimuthally averaged flow occurs within, but near the top of the frictional layer as is commonly observed (Montgomery et al. 2006a, Bell and Montgomery 2008, Zhang et al. 2011, Montgomery et al. 2014; Sanger et al. 2014). This counter-intuitive result occurs despite the tendency for surface stress at the air-sea interface to locally slow down the tangential winds underneath the vortex. The reason is because the strong frictionally-induced inflow can converge M sufficiently rapidly to outweigh the loss of M to the ocean (Smith et al. 2009; Montgomery et al. 2010a; Smith et al. 2014; Kilroy et al. 2017).

The spin-up mechanism associated with frictional stress for realistic values of the drag coefficient and a fully nonlinear boundary layer is referred to as the nonlinear boundary layer spin-up mechanism, although as noted above (and also by Montgomery and Smith 2014, 2017), it is coupled to the conventional spin up mechanism, which is driven by the aggregate diabatic heating of the convection in the central region of the developing vortex and the moist surface enthalpy fluxes that support these convective structures (Rutherford et al. 2012). Recent findings by Montgomery and Persing (2020) and Wang et al. (2021) affirm prior findings of Bui et al. (2009) and Abarca and Montgomery (2014) and refute implications that the strict Eliassen balance model captures the primary characteristic of hurricane intensification in both the interior and boundary layer regions of an intensifying hurricane vortex. The results demonstrate that, for realistic sub-grid-scale parameters consistent with the latest observational guidance, the

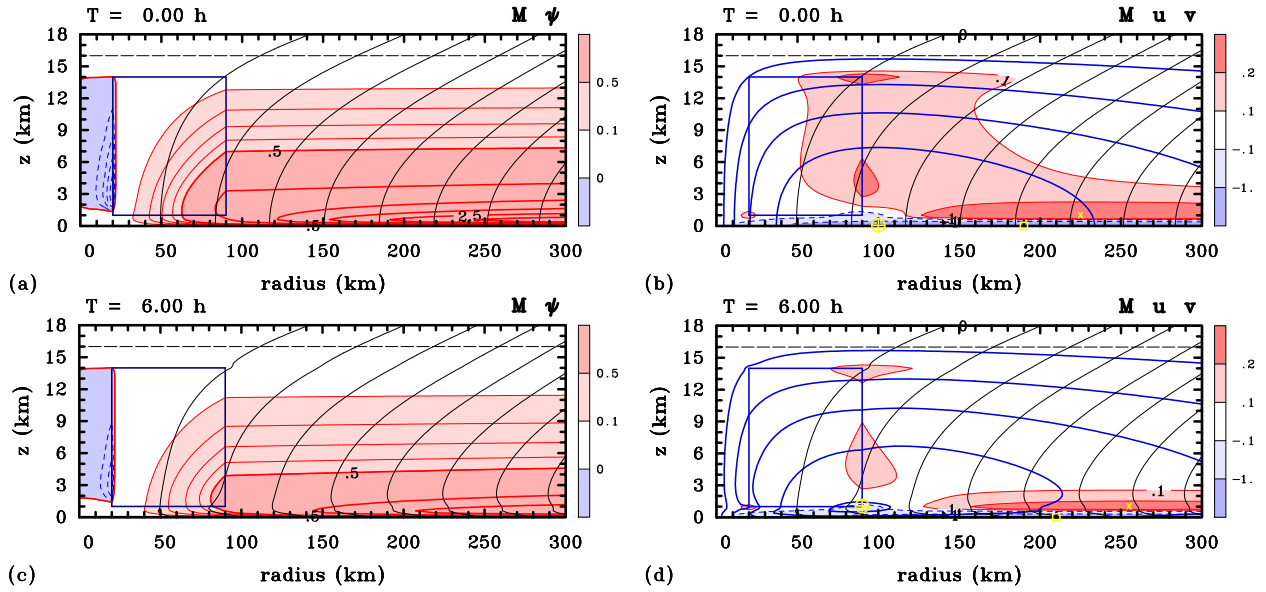


Figure 4. Radial-height cross sections of M -surfaces (thin black curves) superimposed on various quantities for the friction-only simulation, but with the coefficient of the term $\partial^2 \psi / \partial r^2$ in the Eliassen equation multiplied by a factor 0.2 in the rectangular region outlined in dark blue. These quantities include: (a,b) streamlines of the secondary circulation, ψ (red and blue contours and shading); (c,d) contours of tangential velocity, v (blue curves), and radial velocity u (shaded). The upper panels are at the initial time and the lower panels are at 6 h. The dashed horizontal line at a height of 16 km indicates the tropopause. Contour intervals are: for M , $5 \times 10^5 \text{ m}^2 \text{ s}^{-1}$; for ψ , $5 \times 10^7 \text{ kg s}^{-1}$ thick positive contours, $1 \times 10^7 \text{ kg s}^{-1}$ thin positive contours, $2 \times 10^5 \text{ kg s}^{-1}$ negative contours; for v , 2 m s^{-1} . Contours for u are 0.1 m s^{-1} and 0.2 m s^{-1} for positive values, 0.1 and 1 m s^{-1} for negative values. Positive contours are solid, negative contours dashed. The yellow symbols in (a) and (b) indicate the locations of maximum v , (\oplus), maximum u , (\otimes) and minimum u , (\square)

nonlinear boundary layer spinup mechanism is necessary to complete the description of spin up in the boundary layer of an intensifying hurricane in a realistic simulation or reality (Montgomery and Smith 2018, Montgomery and Persing 2020).

The enhancement of the spin up rate by nonlinear boundary layer effects was suggested long ago by Ooyama (1968) and re-affirmed by Smith et al. (2009), Montgomery et al. (2010a), Smith et al. (2014), Schecter (2011) (section 2.2, Fig. 4), Persing et al. (2013) (section 7, Fig. 21), Kilroy et al. (2017) (Fig. 1, sections 5, 8) and Wang et al. (2019) (Fig. 17, sections 4c, 5)⁶.

In summary, the inclusion of a nonlinear boundary layer is necessary to complete the description of spin up in the boundary layer and eyewall of a realistic tropical cyclone and is expected to increase the spin-up rate in comparison to the zero- and first-order models employing a minimal frictional boundary layer as described above. As explained in Section 3, this is because the enhanced near-surface wind speeds will increase values of θ_e entering the central core convection, thereby enhancing the diabatic heating rate and its radial gradient.

⁶Such enhancement appears to have been downplayed by Li and Wang (2021) even though their own results (their Fig. 4) show clearly that a strong drag coefficient *enhances* the spin up rate in comparison to a weak drag coefficient over the first 48 hours!

2.6 Cumulus parameterization in minimal models

Referring back to Case A in Section 2.4.2, it is seen that the explicit representation of latent heat release encapsulated in Eq. (6), in conjunction with the balance vortex formulation as an elliptic problem, implies that the flow above the boundary layer must be everywhere outwards. In Case B, the Eliassen equation becomes hyperbolic in regions of conditional instability. This hyperbolic region is where deep convective clouds would be expected to form. Such clouds would have the ability to reverse the frictionally-induced outflow above the boundary layer, leading to inflow in the lower troposphere, which is necessary to converge absolute angular momentum to facilitate vortex spin up.

Early attempts to simulate tropical cyclones using axisymmetric numerical models were frustrated by the emergence of deep convective clouds instead of a coherent tropical-cyclone-like vortex. A nice review of this work is given by Emanuel (2018), page 15.6. Had these early studies had the computational resources to simulate for a longer time period, they would have likely found a coherent vortex to develop (e.g., Rotunno and Emanuel 1987) even though the deep convective rings that would evolve in the early stages of development are not realistic and give erroneous characteristics and dependencies on the surface drag for example (Persing et al. 2013). As is well known to forecasters, in these stages, deep convection is generally localized and highly asymmetric.

Since the early modelling studies lacked the computational ability to resolve deep convective clouds, parameterization schemes were developed to represent such clouds as sub-grid-scale phenomena, not only for idealized studies in the Tropics, but more generally for numerical weather prediction and climate models. Thus many of the early minimal models for tropical cyclones saw the need to include a parameterization scheme for deep cumulus clouds: examples include Ooyama (1968), Ooyama (1969), Emanuel (1989), Zhu et al. (2001), Nguyen et al. (2002). An important feature of these schemes was to facilitate a pattern of low-level convergence and upper-level divergence in regions of deep convection enabling the natural tendency for frictionally-driven outflow above the boundary layer to be reversed. Interestingly, the early Ooyama models listed above and that of Emanuel (1989) included a parameterization scheme for deep convection that would serve such a purpose, placing it in the category of Case B in Section 2.4.2, while the later Emanuel models, e.g., Emanuel (1995), Emanuel (1997) and Emanuel (2012) appear to fall into the category of Case A, where radial outflow is present above the boundary layer (see, e.g., Emanuel 1995, Fig. 1; Emanuel 1997, Fig. 5; Montgomery and Smith 2019, Fig. 1)⁷. It would be reasonable to ask, then, what is the physics of spin up in these later models?

The bottom line is that, in order to incorporate the physics embodied in the classical spin up mechanism, one needs to implement a parameterization scheme for deep cumulus convection. This remark is appropriate, in particular, to Case B of the first-order model outlined in Section 2.3.

3 Role of the WISHE feedback?

In a seminal paper, Malkus and Riehl (1960) developed the idea that the near-surface θ_e , say θ_{eb} , needs to become elevated as air parcels move inwards in the thermodynamic boundary layer. Assuming a vanishing perturbation pressure at an altitude of 100 mb and supposing that in the deep-convective eyewall region, $\theta_e^* = \theta_{eb}$, they used the hydrostatic equation to derive a relationship between the surface pressure deficit and the increase of θ_{eb} with decreasing radius at the base of the eyewall:

$$\delta p_s = -2.5\delta\theta_{eb} \quad (11)$$

⁷The analysis in Section 2.4.2 calls into question a statement made in our review of paradigms for tropical cyclone intensification (Montgomery and Smith 2014) concerning the Emanuel 1997 (E97) theory. There, on page 48, we said: “The effects of latent heat release in clouds are implicit also in the E97 model, but the negative radial gradient of θ_e in the boundary layer is roughly equivalent to a negative radial gradient of diabatic heating in the interior, which, according to the balance concepts discussed earlier in ‘The overturning circulation’ will lead to an overturning circulation with inflow in the lower troposphere”. The more in-depth analysis of the Eliassen equation underpinning Case A above suggests that this is not the case. Thus, we are led to retract the statement that “the spin-up above the boundary layer (in E97) is entirely consistent with that in Ooyama’s cooperative intensification theory.”

where δp_s is the surface pressure drop in millibars, and $\delta\theta_{eb}$ is the increase in θ_{eb} (in Kelvin) at the inside of the eyewall cloud.

An important feature of the Emanuel models for vortex intensification is the recognition that deep convection outside the central cumulus zone and in rainbands in the outer region of the vortex will produce convective downdraughts that tend to lower θ_{eb} . Of course, the surface enthalpy fluxes act to increase θ_{eb} and to counter the dilution due to downdraughts. As the central cumulus zone is approached from the outside, the air throughout the troposphere will become progressively moistened by deep convection so that downdraughts will become weaker. At the same time, the near-surface winds will increase. As long as the increase of sea surface enthalpy flux with wind speed is not outweighed by a decrease in the thermodynamic disequilibrium at the sea surface in the aerodynamic flux formula, the enthalpy fluxes will increase, leading to an increase in θ_{eb} with decreasing radius. In fact, at a given time, the decreasing surface pressure with decreasing radius will serve to increase the saturation mixing ratio, r^* , which would help to maintain the degree of thermodynamic disequilibrium, an effect argued to be important by Ooyama (1969).

Recalling the approximate formula for \dot{Q} given by Equation (6), and its proportionality with $\dot{\theta}$ and attendant forcing in the Eliassen equation (3), we would expect to find a negative radial gradient of \dot{Q} in the core region as the inflowing air ascends to feed the eyewall clouds while materially conserving its θ_e^* , the proviso being that w_{max} does not weaken with decreasing radius. This caveat regarding w_{max} seems hardly necessary, however, since according to the Eliassen balance theory as exemplified by the zero-order models, a negative radial gradient of \dot{Q} (and corresponding negative radial gradient of $\dot{\theta}$), would lead to a deep overturning circulation in which the vertical profile of w progressively increases with decreasing radius. Such an increase is supported by the explicit calculations shown in Figs. 1 and 3 and in Smith et al. (2018a), see e.g. their Figs. 3e,f and Figs. 6c,e.

Given the balance model formulation developed above in conjunction with the necessary cumulus parameterization, it is of interest to interpret the purported WISHE feedback mechanism in terms of the prognostic balance model reviewed in Section 2.1. The essence of the WISHE theory would appear to be that an increase of the tangential winds with time *is the result of* the increase in the surface enthalpy fluxes with time, which, in turn, increase with near-surface wind speed. However, as noted in the Introduction, the mechanism by which the increase in the surface enthalpy fluxes lead to an increase of the tangential winds remains to be articulated satisfactorily. Indeed, according to the first-order model with some suitable parameterization of deep convection, as long as the surface fluxes maintain a deep overturning circulation with inflow in the lower troposphere, and, as long as the air converging in the boundary layer can be ventilated by inner-core deep convection to the upper troposphere, the vortex will continue to intensify. In

this sense there is no need for coupling between the increasing surface enthalpy fluxes and the increase in the tangential wind speed.

It is now easy to see using the first-order model, with a suitable parameterization scheme for deep convection, how a temporal increase of the surface fluxes will lead to an increase in the intensification rate and maximum intensity of the vortex. If the surface enthalpy fluxes increase with time, the increase of θ_{eb} will be augmented relative to a simulation in which surface flux distribution is held constant-in-time. Provided that the increased θ_{eb} associated with the increased surface flux increases the areally-integrated vertical mass flux of the convection in the developing eye-wall updraught, the increased surface flux will augment the strength of the secondary circulation, the rate of intensification and the maximum attainable tangential wind. From the perspective of the first-order model, and subject to the foregoing caveats, the feedback associated with the increase of the surface fluxes with time will augment the intensification rate and the maximum intensity in real world situations.

The foregoing conclusion supports the numerical modeling results of [Nguyen et al. \(2008\)](#), [Montgomery et al. \(2009\)](#), [Montgomery et al. \(2015\)](#) and later experiments of [Zhang and Emanuel \(2016\)](#), all of whom showed that the intensification rate is most rapid and the maximum intensity is greatest when the wind-speed dependence of the surface fluxes is retained.

4 Important caveats

In the foregoing conceptual models for intensification, we have described the key elements contributing to the spin up of the maximum tangential winds. However, there are several important caveats that we glossed over for expediency, but which should be noted for completeness. Some are relatively obvious consequences of the balance model formulation, but others are more subtle, transcending the balance model framework and requiring careful consideration in specific implementations of the conceptual models presented.

- (1) From explicit solutions to the zero-order model, within a relatively short space of time, on the order of half a day for the model parameters chosen for the [Smith et al.](#) study, the M -surfaces fold over in the upper-troposphere and regions of inertial instability develop. In these regions, the Eliassen equation for the streamfunction of the overturning circulation becomes hyperbolic and strict balance solutions beyond this time are possible only if the coefficients of the equation are modified (or regularized) to remove the unstable region. However, this procedure does not eliminate instability completely and is only a temporary fix. This is because the prognostic equation for the tangential wind component still contains a term involving the negative radial gradient
- of M . Indeed, after another half a day, the solution breaks down completely. The development of such unstable regions in the upper troposphere is a robust feature of three-dimensional model simulations (e.g., [Wang et al. 2020](#), Figs. 2c, 2e; [Wang et al. 2021](#), Fig 2; [Montgomery and Persing 2020](#), Fig. 4) and in this sense the balance solutions are weak solutions and the details of the predicted flow in these regions should be taken *cum grano salis*.
- (2) The later Emanuel models conceived to underpin the WISHE feedback mechanism have the topology of the M -surfaces near the radius of maximum gradient wind hard-wired to ascend to the upper troposphere and flare out to large radius without bending downward or overturning. This assumption has the unintended effect of preventing the development of inertially unstable regions. It precludes also the possibility of layers of inflow developing above and below the upper tropospheric outflow layer, a feature commonly exhibited in modelling studies ([Rotunno and Emanuel 1987](#); [Montgomery et al. 2020](#); [Wang et al. 2020](#)). Perhaps more importantly, as noted in Section 2.6, the [Emanuel \(1995\)](#), [Emanuel \(1997\)](#) and [Emanuel \(2012\)](#) axisymmetric balance models appear to fall in the category of Case A in Section 2.4.2: they do not include a parameterization of deep cumulus convection that would allow the classical spin up mechanism to be a feature of the dynamics.
- (3) The intensification process as sketched in Sections 2.2 and 2.4 assumes that the maximum tangential (gradient) wind, V_{max} , amplifies with time, the idea being that the diabatically-driven overturning circulation draws M surfaces inwards at or near the radius of maximum tangential wind. This assumption is consistent with the classical [Shapiro and Willoughby](#) explanation.
- (4) In the first-order model, it is presumed that deep convection is strong enough to carry moist air into the upper troposphere. When surface friction is taken into account in the explanation, the deep secondary circulation produced by the diabatic heating would need to be strong enough to ventilate the moist air that is converging in the boundary layer. However, this ventilation cannot be taken for granted ([Smith and Wang 2018](#); [Smith et al. 2021](#)). In contrast, as noted above, in the [Emanuel 1997](#) and [2012](#) models, all air converging in the boundary layer is constrained to ascend to the upper troposphere.
- (5) To initiate and maintain deep convection in the inner-core region, it is necessary that θ_{eb} be high enough to main convective instability. Such an elevation of boundary layer θ_{eb} can only come about through moist enthalpy fluxes at the sea surface and these fluxes must outweigh the adverse effect of frictionally induced and mesoscale and convective downdraughts that transport cool dry air into the boundary layer. The crucial role of the entropy fluxes is then to

maintain deep convective instability in the face of the frictional subsidence and downdraughts. This role was importantly recognized by Emanuel (1986); Rotunno and Emanuel (1987); Emanuel (1989).

- (6) In the foregoing analysis it has been presumed that the bulk of the vortex dynamics and thermodynamics are governed to zero order by azimuthally-averaged flow quantities relative to a nominal, slowly-varying, center of circulation. At the very early stages of development, an appropriate center of circulation is often given by the “sweet spot” of the marsupial pouch of an easterly wave or disturbance in the monsoon trough, which has been demonstrated to be a robust “attractor point” for the eventual convective-vorticity organization in both real-world and idealized circumstances (Dunkerton et al. 2009, Montgomery et al. 2010b, Wang et al. 2012, Asaadi et al. 2017). Our focus here on the azimuthally-averaged dynamics relative to this center does not imply, however, that the eddy (non-axisymmetric) terms are negligible. Indeed, the azimuthal mean convective heating rate is often dominated by the integral over the localized deep convective structures in the cumulus zone of the incipient vortex (e.g. Montgomery et al. 2006b; Smith et al. 2015, Fig. 8; Persing et al. 2013, Fig. 5c.). What’s more, local variability in the thermodynamic disequilibrium between the ocean and the atmosphere (primarily associated with saturated specific humidity at the SST over warm oceanic features) may furnish important contributions to the mean buoyancy forcing of deep convective structures in the inner-core region during rapid intensification events (Jaimes et al. 2015). The azimuthally-averaged vertical transport of eddy tangential and radial momentum may play a significant quantitative role in the ensuing intensification of the system-scale vortex also (e.g., Persing et al. 2013, Montgomery et al. 2020). All of this is just a reminder that the proper benchmark of a spin up theory is a three-dimensional configuration for the atmosphere and ocean and the present formulation focuses on the strictly axisymmetric atmospheric dynamics for simplicity. In specific circumstances, the eddy covariance terms may be comparable to or even dominate the strictly mean terms in the inner-core region of the vortex and would need to be included explicitly in the foregoing analyses.

5 Implications for recent work

As foreshadowed in the Introduction, we return here to appraise the study by Zhu et al. (2021), which invokes a “kicking off” of a “WISHE-like positive feedback mechanism” to explain the differences between two highlighted simulations of Hurricane Michael (2018), one with an improved representation of sub-grid-scale turbulence.

On p17 they show that a key difference in the simulation using the improved scheme is the larger influx of cyclonic absolute vorticity in the planetary boundary layer. They argue that the large positive tangential wind tendency implied by this influx of cyclonic vorticity and “the resultant increase of tangential wind enhance surface evaporation and radial convergence of moisture in the PBL ..., which further fosters stronger eyewall convection evidenced from the increase of vertical velocity The enhanced eyewall convection in turn causes the further increase of radial inflow”

In contrast, in the old model, the positive wind tendency associated with the influx of vorticity is found to remain relatively weak and insufficient to “generate the needed acceleration of tangential wind to kick off the WISHE-like feedback mechanism underlying the RI (rapid intensification, our insertion) of Michael”. In the new model, the presumed chain of effects listed in the foregoing description is thought to be an affirmation of the initiation of the purported WISHE mechanism. However, in view of the results presented herein, the conflation of these effects with a WISHE feedback seems a little rash to us.

The question remains whether a similar result would emerge had the surface heat fluxes been frozen in time during the RI period. Certainly, an increase of tangential wind will lead through boundary layer dynamics to an increase in the boundary layer inflow and to an increase in the radial convergence of moisture even if the fluxes are frozen in time. Another point to consider is the proposed link between the increased moisture convergence and the stronger eyewall convection as evidenced by the increase of azimuthally-averaged vertical velocity at the 900 hPa level. However, an increased vertical velocity at this level does not guarantee an increase in the mean convective mass flux in the middle troposphere. It could happen that the increased boundary layer inflow could not be all ventilated by the developing eyewall convection.

Our own experience with idealized calculations has suggested that the ventilation of the boundary layer inflow is often accomplished during the early phase of intensification (Kilroy et al. 2016, Smith and Wang 2018, Smith et al. 2021), but in real-world cases it should not be taken for granted that all the mass being funneled to the base of the eyewall by the boundary layer will be ventilated by the convection. In fact, moisture convergence *per se* is the wrong quantity to examine, since, as discussed in Section 3, the equivalent potential temperature of the boundary layer θ_{eb} is arguably the more relevant quantity. Hence the presumed linkage between moisture convergence and convective strength seems tenuous.

All else being equal, one might plausibly associate an increase in θ_{eb} with an increase in local buoyancy in the developing eyewall and thus an increase in the local mean vertical velocity. However, the *effective buoyancy* and therefore the vertical acceleration it produces depends *inter alia* on the horizontal scale of the updraught (Smith and Montgomery 2022). Even if the vertical gradient of the

saturation mixing ratio were unchanged, an increase in the mean vertical velocity would, according to Eq. (6), imply an increase in the mean heating rate \dot{Q} and its associated radial gradient. According to the balance model of Section 2.1, an increased magnitude of $\partial\dot{Q}/\partial r$ would imply a strengthening of the overturning circulation and hence an increased spin up tendency of mean tangential velocity via the increased mean influx of cyclonic absolute vorticity.

In a related issue, the authors suggest on p17 (also p21) that: “regardless of the strength of individual convective elements the azimuthal-mean eyewall convection must exceed a critical level so that the induced mean secondary overturning circulation can generate sufficiently large inward transport of absolute vorticity needed for vortex intensification.” We are perplexed about the meaning of this suggestion because as long as there is mean inflow above the boundary layer the vortex will intensify. Why is a critical level of radial influx of cyclonic vorticity necessary to initiate intensification?

In summary: We applaud work examining the primary reason for improved forecasts of the rapid intensification of a tropical cyclone threatening coastal communities and marine assets. It is hoped that the foregoing discussion will contribute to continued efforts towards identifying the primary mechanisms of the rapid intensification of Hurricane Michael and other real-world tropical cyclones.

6 Conclusions

We have examined a hierarchy of minimal conceptual models for tropical cyclone intensification because popular explanations of intensification still appear to invoke the imprecisely articulated WISHE feedback process. The conceptual models are framed mostly in terms of axisymmetric balance dynamics as the feedback process is traditionally presented using balance constraints.

In the first set of models, i.e., the zero-order models, the heating rate is prescribed and taken to be constant with time in such a way to mimic a deep overturning circulation with convergence in the lower troposphere and divergence in the upper troposphere. The solutions indicate that as long as convective instability is maintained by the surface enthalpy fluxes in the central region, vortex intensification does not require the surface enthalpy fluxes to increase with time. The structure of the latent heating rate is assumed to have a maximum in the middle troposphere to ensure that the aggregate of convective clouds in the central zone of the developing vortex draws absolute angular momentum surfaces inwards in the lower troposphere and above the boundary layer.

In the second set of models, i.e., the first-order models, the heating rate is related explicitly to the latent heat release of ascending convective elements that first saturate in the upper boundary layer, which, depending on the thermodynamic properties of ascending air, may or may not reach the upper troposphere. As is well known, the release

of latent heat markedly reduces the local static stability of rising air. In the balance framework, two possibilities are conceivable.

The first possibility is that the effective (moist) static stability and the related discriminant in the Eliassen equation for the overturning circulation in saturated air, although small, remains positive. In this case, the solution is essentially that of a moist-saturated vortex spin down problem in which the rising air in the central region flows radially outwards in a comparatively deep layer which, in turn, leads to a rapidly decreasing tangential wind component on account of the conservation of absolute angular momentum above the boundary layer.

The second possibility is that the effective static stability and related discriminant in the Eliassen equation in saturated air is negative. We believe this is the more likely possibility during vortex intensification since locally the air is conditionally unstable in the central area of the developing vortex. In such regions, where the stability and corresponding discriminant is negative, the Eliassen equation is hyperbolic. In unstable regions, air parcels would be able to accelerate vertically under their local buoyancy so that the hydrostatic approximation and therefore thermal wind balance will break down. The breakdown of the formulation as a globally elliptic problem is an indication that localized buoyant deep convection is seeking to develop. Under these circumstances, deep convection would need to be parameterized in order to proceed with the balance formulation. Once again, like the zero-order model, in order for the model to capture vortex spin up, it is necessary that the convective parameterization possess the property that the cumulus mass flux achieve its maximum in the middle troposphere so that the parameterized clouds draw absolute angular momentum surfaces inwards in the lower troposphere and above the boundary layer.

The foregoing findings help to understand the differences between the early Ooyama models of 1968 and 1969 and the Emanuel models of 1989, 1995, 1997 and 2012. Emanuel’s 1989 model appears to fit into this second possibility, whereas the subsequent models of 1995, 1997 and 2012 appear to fit into the first possibility. Our reasoning to support these interpretations is that the 1989 model has a parameterization of cumulus convection with a mass flux that increases with height, allowing for the possibility of driving a deep overturning circulation as in the zero-order model described herein. The lower tropospheric inflow associated with this circulation reverses the outflow forced by boundary layer friction. From our interpretation of Emanuel’s cartoons presented in 1995, 1997, 2012 and/or corresponding mathematical formulations, the radial flow is everywhere outwards above the boundary layer and there appears to be no mechanism to draw angular momentum surfaces inwards to spin up the vortex above the boundary layer.

The minimal models, along with previously published explicit solutions, re-affirm previous findings that vortex intensification does not necessarily require the surface

enthalpy fluxes to increase with time, but only that these fluxes are sufficient to maintain convective instability and a deep region of latent heating with a negative radial gradient. This latter condition requires also that the heating rate increase with height to the middle troposphere to ensure that the latent heat forcing associated with the aggregate of convective clouds in the cumulus zone of the developing vortex draws absolute angular momentum surfaces inwards above the boundary layer.

From the perspective of the first-order model, we can now answer the question posed in the Introduction regarding popular explanations of the WISHE feedback mechanism. If the surface enthalpy fluxes increase with time, the increase of moist equivalent potential temperature in the boundary layer will be augmented relative to formulations that do not allow the fluxes to increase with time. Provided that the increased boundary layer equivalent potential temperature associated with the increased surface flux increases the areally-integrated vertical mass flux of the convection in the developing eyewall updraught, the increased surface flux will augment the strength of the secondary circulation, the rate of intensification and the maximum attainable tangential wind. Thus, subject to the foregoing caveats, we now see how the feedback associated with the increase of the surface fluxes with time augments the intensification rate and the maximum intensity in real world situations.

Longer-term solvability issues that arise in the solution of the minimal balance models are a reminder of the weakness of strict axisymmetric balance models when formulated for evolutionary studies of tropical cyclone intensification. A further weakness, of course, is the fact that the boundary layer, itself, is generally not close to gradient wind balance, especially in the inner vortex region. The nonlinear boundary layer spinup mechanism is generally necessary to complete the description of spinup in the boundary layer and eyewall of an intensifying hurricane. Notwithstanding these limitations, the minimal balance model framework has helped provide new insights.

Some implications for recent work were discussed.

Acknowledgements

This work was inspired by a stimulating discussion with tropical cyclone researchers and forecasters on the Tropical Storms List in 2021 and we thank all participants in that discussion, including Mark Lander, who initiated the discussion. A special thanks goes to Minhee Chang, Michael Reeder and Michael Riemer for their perceptive comments on the first draft of the manuscript and to Frank Marks for his review of the second draft.

MTM acknowledges the support of NSF grant IAA-1656075, ONR grant N0001417WX00336, and the U. S. Naval Postgraduate School. The views expressed herein are those of the authors and do not represent sponsoring agencies or institutions.

References

- Abarca, S. F. and M. T. Montgomery, 2014: Departures from axisymmetric balance dynamics during secondary eyewall formation. *J. Atmos. Sci.*, **71**, 3723–3738.
- Anthes, R. A., 1974: The dynamics and energetics of mature tropical cyclones. *Rev. Geophys. Space Phys.*, **12**, 495–522.
- Asaadi, A., G. Brunet, and M. K. Yau, 2017: The importance of critical layer in differentiating developing from nondeveloping easterly waves. *J. Atmos. Sci.*, **74**, 409–417.
- Bell, M. M. and M. T. Montgomery, 2008: Observed structure, evolution, and potential intensity of Category 5 Hurricane Isabel (2003) from 12 to 14 September. *Mon. Wea. Rev.*, **136**, 2023–2046.
- Bui, H. H., R. K. Smith, M. T. Montgomery, and J. Peng, 2009: Balanced and unbalanced aspects of tropical-cyclone intensification. *Quart. Journ. Meteor. Soc.*, 1715–1731.
- Carrió, D. S., V. Homar, A. Jansa, R. Romero, and M. A. Picornell, 2017: Tropicalization process of the 7 November 2014 Mediterranean cyclone: Numerical sensitivity study. *Atmos. Res.*, **197**, 300–312.
- Dunkerton, T. J., M. T. Montgomery, and Z. Wang, 2009: Tropical cyclogenesis in a tropical wave critical layer: easterly waves. *Atmos. Chem. Phys.*, 5587–5646.
- Emanuel, K., 2005: Genesis and maintenance of “Mediterranean hurricanes”. *Adv. Geosciences*, **2**, 217–220.
- Emanuel, K. A., 1986: An air-sea interaction theory for tropical cyclones. Part I: Steady state maintenance. *J. Atmos. Sci.*, **43**, 585–604.
- 1989: The finite amplitude nature of tropical cyclogenesis. *J. Atmos. Sci.*, **46**, 3431–3456.
- 1995: Behaviour of a simple hurricane model using a convective scheme based on subcloud-layer entropy equilibrium. *J. Atmos. Sci.*, **52**, 3960–3968.
- 1997: Some aspects of hurricane inner-core dynamics and energetics. *J. Atmos. Sci.*, **54**, 1014–1026.
- 2003: Tropical cyclones. *Annu. Rev. Earth Planet. Sci.*, **31**, 75–104.
- 2012: Self-stratification of tropical cyclone outflow. Part II: Implications for storm intensification. *J. Atmos. Sci.*, **69**, 988–996.
- 2018: 100 years of progress in tropical cyclone research. *Meteorological Monographs*, **59**, 15.1–15.68.
- 2019: Inferences from simple models of slow, convectively coupled processes. *J. Atmos. Sci.*, **76**, 195–208.
- Emanuel, K. A., J. D. Neelin, and C. S. Bretherton, 1994: On large-scale circulations of convecting atmospheres. *Quart. Journ. Roy. Meteor. Soc.*, **120**, 1111–1143.
- Greenspan, H. P. and L. N. Howard, 1963: On a time-dependent motion of a rotating fluid. *J. Fluid Mech.*, **17**, 385–404.
- Jaimes, B., L. K. Shay, and E. Uhlhorn, 2015: Enthalpy and momentum fluxes during Hurricane Earl relative to underlying ocean features. *Mon. Wea. Rev.*, **143**, 111–131.

- Kilroy, G., M. T. Montgomery, and R. K. Smith, 2017: The role of boundary layer friction on tropical cyclogenesis and subsequent intensification. *Q. J. R. Meteorol. Soc.*, **143**, 1–15.
- Kilroy, G., R. K. Smith, and M. T. Montgomery, 2016: Why do model tropical cyclones grow progressively in size and decay in intensity after reaching maturity? *J. Atmos. Sci.*, **73**, 487–503.
- Kilroy, G., H. Zhu, M. Chang, and R. K. Smith, 2022: Application of the rotating-convection paradigm for tropical cyclones to interpreting medicanes: an example. *Submitted to Trop. Cycl. Res. Rev.*, **11**, 1–15.
- Li, T. and Y. Wang, 2021: The role of boundary layer dynamics in tropical cyclone intensification. Part I: Sensitivity to surface drag coefficient. *J. Meteorol. Soc. Japan*, **99**, 537–554.
- Malkus, J. S. and H. Riehl, 1960: On the dynamics and energy transformations in steady-state hurricanes. *Tellus*, **12**, 1–20.
- Miglietta, M. M., D. Carnevale, V. Levizzani, and R. Rotunno, 2020: Role of moist and dry air advection in the development of mediterranean tropical-like cyclones (medicanes). *Quart. Journ. Roy. Meteor. Soc.*, **146**, 876–899.
- Miglietta, M. M. and R. Rotunno, 2019: Development mechanisms for mediterranean tropical-like cyclones (medicanes). *Quart. Journ. Roy. Meteor. Soc.*, **145**, 1444–1460.
- Montgomery, M. T., M. M. Bell, S. D. Aberson, and M. L. Black, 2006a: Hurricane Isabel (2003): New insights into the physics of intense storms. Part I mean vortex structure and maximum intensity estimates. *Bull. Amer. Meteor. Soc.*, **87**, 1335–1348.
- Montgomery, M. T., G. Kilroy, R. K. Smith, and N. Črnivec, 2020: Contribution of mean and eddy momentum processes to tropical cyclone intensification. *Quart. Journ. Roy. Meteor. Soc.*, **146**, 3101–3117.
- Montgomery, M. T., S. V. Nguyen, R. K. Smith, and J. Persing, 2009: Do tropical cyclones intensify by WISHE? *Quart. Journ. Roy. Meteor. Soc.*, **135**, 1697–1714.
- Montgomery, M. T., M. E. Nichols, T. A. Cram, and A. B. Saunders, 2006b: A vortical hot tower route to tropical cyclogenesis. *J. Atmos. Sci.*, **63**, 355–386.
- Montgomery, M. T. and J. Persing, 2020: Does balance dynamics well capture the secondary circulation and spin-up of a simulated tropical cyclone? *J. Atmos. Sci.*, **78**, 75–95.
- Montgomery, M. T., J. Persing, and R. K. Smith, 2015: Putting to rest WISHE-ful misconceptions. *J. Adv. Model. Earth Syst.*, **07**, doi:10.1002/.
- 2019: On the hypothesized outflow control of tropical cyclone intensification. *Q. J. R. Meteorol. Soc.*, **145**, 1303–1322.
- Montgomery, M. T. and R. K. Smith, 2014: Paradigms for tropical cyclone intensification. *Aust. Met. Ocean. Soc. Journl.*, **64**, 37–66.
- 2017: Recent developments in the fluid dynamics of tropical cyclones. *Annu. Rev. Fluid Mech.*, **49**, 541–574.
- 2018: Comments on: Revisiting the balanced and unbalanced aspects of tropical cyclone intensification, by J. Heng, Y. Wang and W. Zhou. *J. Atmos. Sci.*, **75**, 2491–2496.
- 2019: Toward understanding the dynamics of spinup in Emanuel’s tropical cyclone model. *J. Atmos. Sci.*, **76**, 3089–3093.
- Montgomery, M. T., R. K. Smith, and S. V. Nguyen, 2010a: Sensitivity of tropical cyclone models to the surface drag coefficient. *Q. J. R. Meteorol. Soc.*, **136**, 1945–1953.
- Montgomery, M. T., Z. Wang, and T. J. Dunkerton, 2010b: Coarse, intermediate and high resolution numerical simulations of the transition of a tropical wave critical layer to a tropical storm. *Atmos. Chem. Phys.*, **10**, 10803–10827.
- Montgomery, M. T., J. Zhang, and R. K. Smith, 2014: An analysis of the observed low-level structure of rapidly intensifying and mature Hurricane Earl (2010). *Q. J. R. Meteorol. Soc.*, **141**, 2132–2146.
- Muller, C. J. and D. M. Romps, 2018: Acceleration of tropical cyclogenesis by self-aggregation feedbacks. *Proc. Natl. Acad. Sci.*, **115**, 2930–2935.
- Nguyen, C. M., R. K. Smith, H. Zhu, and W. Ulrich, 2002: A minimal axisymmetric hurricane model. *Quart. Journ. Roy. Meteor. Soc.*, **128**, 2641–2661.
- Nguyen, V. S., R. K. Smith, and M. T. Montgomery, 2008: Tropical-cyclone intensification and predictability in three dimensions. *Q. J. R. Meteorol. Soc.*, **134**, 563–582.
- Ooyama, K. V., 1968: Numerical simulation of tropical cyclones with an axi-symmetric model. *New York University Technical Report*, 1–8.
- 1969: Numerical simulation of the life cycle of tropical cyclones. *J. Atmos. Sci.*, **26**, 3–40.
- Persing, J., M. T. Montgomery, J. McWilliams, and R. K. Smith, 2013: Asymmetric and axisymmetric dynamics of tropical cyclones. *Atmos. Chem. Phys.*, **13**, 12299–12341.
- Rogers, R. F., S. Aberson, M. Black, P. Black, J. Cione, P. Dodge, J. Dunion, J. Gamache, J. Kaplan, M. Powell, N. Shay, N. Surgi, and E. Uhlhorn, 2006: The Intensity Forecasting Experiment: A NOAA multiyear field program for improving tropical cyclone intensity forecasts. *Bull. Amer. Meteor. Soc.*, **87**, 1523–1537.
- Rotunno, R. and K. A. Emanuel, 1987: An air-sea interaction theory for tropical cyclones. Part II Evolutionary study using a nonhydrostatic axisymmetric numerical model. *J. Atmos. Sci.*, **44**, 542–561.
- Ruppert, J. H., A. A. Wing, X. Tang, and E. L. Duran, 2020: The critical role of cloud–infrared radiation feedback in tropical cyclone development. *Proc. Natl. Acad. Sci.*, **45**, 27884–27892.
- Rutherford, B., G. Dangelmayr, and M. T. Montgomery, 2012: Lagrangian coherent structures in tropical cyclone intensification. *Atmos. Chem. Phys.*, **12**, 5483–5507.
- Sanger, N. T., M. T. Montgomery, R. K. Smith, and M. M. Bell, 2014: An observational study of tropical-cyclone spin-up in Supertyphoon Jangmi (2008) from 24 - 27 September. *Mon. Wea. Rev.*, **142**, 3–28.
- Schecter, D. A., 2011: Evaluation of a reduced model for investigating hurricane formation from turbulence. *Q. J. R. Meteor. Soc.*, **137**, 155–178.
- Schubert, W. H. and J. J. Hack, 1982: Inertial stability and tropical cyclone development. *J. Atmos. Sci.*, **39**, 1687–1697.
- Shapiro, L. J. and H. Willoughby, 1982: The response of balanced hurricanes to local sources of heat and momentum. *J. Atmos. Sci.*, **39**, 378–394.

- Smith, R. K., 2006: Accurate determination of a balanced axisymmetric vortex. *Tellus A*, **58**, 98–103.
- Smith, R. K., G. Kilroy, and M. T. Montgomery, 2015: Why do model tropical cyclones intensify more rapidly at low latitudes? *J. Atmos. Sci.*, **72**, 1783–1804.
- 2021: Tropical cyclone life cycle in a three-dimensional numerical simulation. *Quart. Journ. Roy. Meteor. Soc.*, **147**, 1111–2222.
- Smith, R. K. and M. T. Montgomery, 2008: Balanced depth-averaged boundary layers used in hurricane models. *Quart. Journ. Roy. Meteor. Soc.*, **134**, 1385–1395.
- 2016: Understanding hurricanes. *Weather*, **71**, 219–223.
- 2022: Effective buoyancy and CAPE: Some implications for tropical cyclones. *Q. J. R. Meteorol. Soc.*, **148**, 1–14.
- Smith, R. K., M. T. Montgomery, and H. Bui, 2018a: Axisymmetric balance dynamics of tropical cyclone intensification and its breakdown revisited. *J. Atmos. Sci.*, **75**, 3169–3189.
- Smith, R. K., M. T. Montgomery, and G. Kilroy, 2018b: The generation of kinetic energy in tropical cyclones revisited. *Quart. Journ. Roy. Meteor. Soc.*, **144**, 2481–2490.
- Smith, R. K., M. T. Montgomery, and S. V. Nguyen, 2009: Tropical cyclone spin up revisited. *Quart. Journ. Roy. Meteor. Soc.*, **135**, 1321–1335.
- Smith, R. K., M. T. Montgomery, and G. L. Thomsen, 2014: Sensitivity of tropical cyclone models to the surface drag coefficient in different boundary-layer schemes. *Q. J. R. Meteorol. Soc.*, **140**, 792–804.
- Smith, R. K. and S. Wang, 2018: Axisymmetric balance dynamics of tropical cyclone intensification: Diabatic heating versus surface friction. *Quart. J. Roy. Meteor. Soc.*, **144**, 2350–2357.
- Sundqvist, H., 1970a: Numerical simulation of the development of tropical cyclones with a ten-level model. Part I. *Tellus*, **4**, 359–390.
- 1970b: Numerical simulation of the development of tropical cyclones with a ten-level model. Part II. *Tellus*, **5**, 505–510.
- Wang, S., M. T. Montgomery, and R. K. Smith, 2021: Solutions of the Eliassen balance equation for inertially and/or symmetrically stable and unstable vortices. *Q. J. R. Meteorol. Soc.*, **147**, 1–12.
- Wang, S. and R. K. Smith, 2019: Consequences of regularizing the Sawyer–Eliassen equation in balance models for tropical cyclone behaviour. *Q. J. R. Meteorol. Soc.*, **145**, 1–14.
- Wang, S., R. K. Smith, and M. T. Montgomery, 2020: Upper-tropospheric inflow layers in tropical cyclones. *Q. J. R. Meteorol. Soc.*, **146**, 3466–3487.
- Wang, Y., C. A. Davis, and Y. Huang, 2019: Dynamics of lower-tropospheric vorticity in idealized simulations of tropical cyclone formation. *J. Atmos. Sci.*, **76**, 707–727.
- Wang, Z., T. J. Dunkerton, and M. T. Montgomery, 2012: Application of the marsupial paradigm to tropical cyclone formation from northwestward-propagating disturbances. *Mon. Wea. Rev.*, **140**, 66–76.
- Wirth, V. and T. J. Dunkerton, 2006: A unified perspective on the dynamics of hurricanes and monsoons. *J. Atmos. Sci.*, **63**, 2529–2547.
- Zhang, F. and K. A. Emanuel, 2016: On the role of surface fluxes and WISHE in tropical cyclone intensification. *J. Atmos. Sci.*, **73**, 2011–2019.
- Zhang, J. A., R. F. Rogers, D. S. Nolan, and F. D. Marks, 2011: On the characteristic height scales of the hurricane boundary layer. *Mon. Wea. Rev.*, **139**, 2523–2535.
- Zhu, H., K. S. R., and W. Ulrich, 2001: A minimal three-dimensional tropical cyclone model. *J. Atmos. Sci.*, **58**, 1924–1944.
- Zhu, P., A. Hazelton, Z. Zhang, F. D. Marks, and V. Tallapragada, 2021: The role of eyewall turbulent transport in the pathway to intensification of tropical cyclones. *J. Geophys. Res. Atmos.*, **126**, 1–26.